From smoking exhaust to clean socket

Design steps from the diesel-powered mobile working machine to the all-electric solution

Part 2 - The triad of battery, motor and inverter

Dr. Armin U. Schmiegel, REFU Drive GmbH, University of Applied Science, Reutlingen

1. Introduction

The electrification of mobile machines makes a significant contribution to reducing environmental pollution. The drivers of this development are not only climate change, but also the observation that electrification can improve the efficiency and precision of machines and processes and additionally support digitalisation. In [1] we described the first design steps for electrification. The main question was which system topology is the right one for a specific application. In further studies, we have illustrated this methodology for various applications. [2], [3].

In this study, we want to address the question of how the battery, motor and inverter are matched to each other. The battery is the energy source, the motor consumes this energy to perform a certain work. Be it the transport of goods or the transport of the machine itself, which then performs work at another location. The inverter is a mediator here, it converts the electrical energy that has been stored in the battery into an electrical field that ensures that the motor provides torque at a certain speed.

2. Battery technology

Batteries are electrochemical storage devices. Their basic function is based on the fact that a voltage is applied and thus a redox reaction takes place. [4], [5]. There are a number of reactions that are suitable for storage. In Table 1 some of them are shown with their efficiencies. η_r are shown. In the electrification of mobile machinery, lithium-ion batteries are the most common. Therefore, we will briefly discuss lithium-ion batteries.

Table 1 : Effect line of various electrochemical storage systems [4]

Chemistry	η_r
lead acid	82%
lithium ion (NMC/LMO)	92%
lithium ion (LFP)	86%
lithium ion (Titanate)	96%
lithium ion (NCA)	92%
high temperature (NAS)	80%
redox flow (Vanadium)	70%
redox flow (ZnBr)	70%

Lithium-ion batteries are a family of electrochemical cells whose basic reaction is very similar. The cathode material consists of a lithium metal oxide, and during the charging or discharging process, some lithium ions are dissolved out of this material, releasing electrons.

$$LiMO_2 \rightleftharpoons Li_{1-x}MO_2 + x\,Li^+ + xe^-$$

Thereby x is the number of lithium ions used in the reaction.

The released electrons have to move to the anode via the terminals of the cell, while the lithium ions move through the separator to the anode. There, lithium ions and electrons are stored.

$$C + xLi^+ + x\,e^- \rightleftharpoons Li_xC$$

In this example, the anode material consists of carbon C.

In lithium-ion batteries, the choice of metal oxide and anode material determines their properties. It has become common to describe the technology in terms of the metal oxide. Lithium iron phosphate batteries, LFP for short, use iron phosphate as the metal oxide. Nickel-manganese-cobalt, NMC for short, use nickel-manganese-cobalt as the metal oxide.

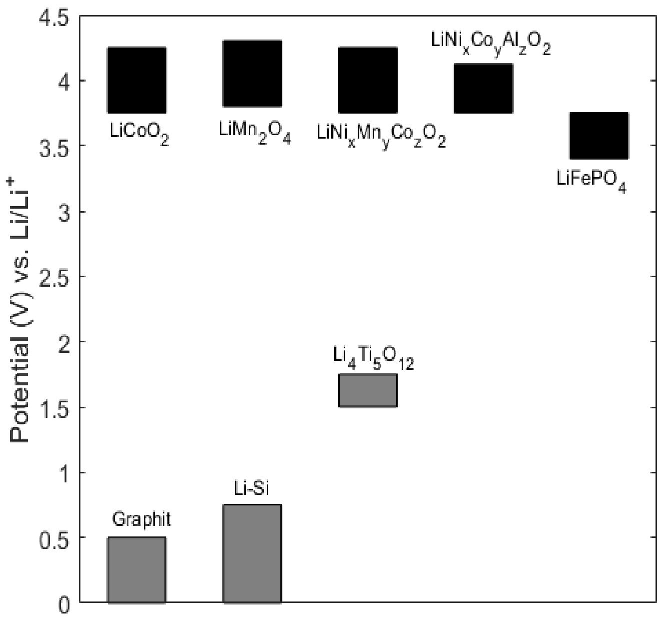

Figure 1 : Potentials of different metal oxides and anode materials.[4], [6]

Different metal oxides and anode materials result in different cell properties and voltages. In Figure 1 shows the electrochemical potentials of lithium metal oxides and anode materials. The difference between the potential of the anode material and the lithium metal oxide corresponds to the voltage range of the cells. As can be seen from Figure 1 the voltage ranges, depending on the combination, are approx. $2V - 3V$ or $3V - 4V$. Which is significantly higher than the electrical potentials of other electrochemical cells.

As we discussed in section 4 we will see, drive applications for mobile machines usually require a significantly higher voltage. To achieve this, several cells are interconnected. There are two options here: Cells can be connected in parallel or in series. The serial connection serves to increase the voltage level. However, a problem arises here that is shown in Figure 2 for NMC and LFP cells.

Although the voltage of the connected cells increases with each additional cell, the voltage window also widens. For example, if 200 NMC cells are connected in series, the voltage window is between $600V$ and $850V$depending on whether the cells are charged or discharged. For LFP cells, the voltage window would be between 510 V and 725 V. It is therefore possible to increase the voltage of the battery by means of a serial connection. However, the voltage window also becomes larger.

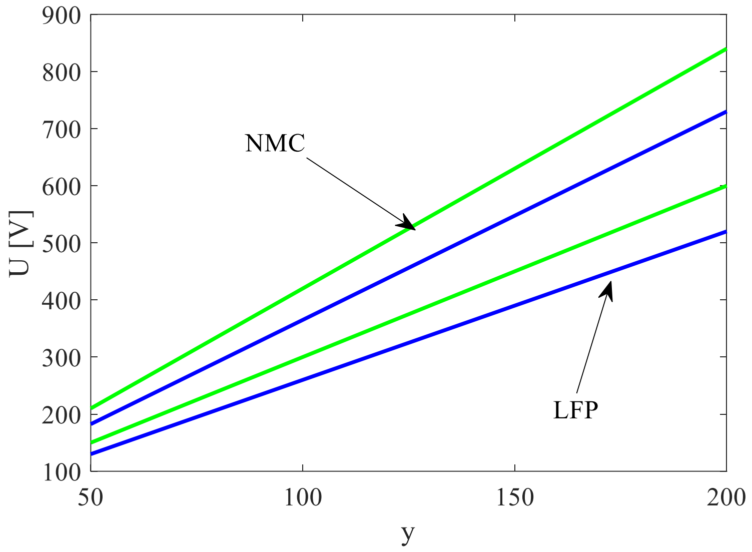

Figure 2 : Voltage window of a lithium-ion battery based on NMC or LFP as cathode material for different interconnections. $1pys$ *interconnections.*

The voltage is determined by the cell chemistry. The maximum power and energy of a cell depend on the active material. As we have seen, during charging and discharging, lithium ions are taken from a lithium metal oxide and stored in the anode material. The amount of active material thus determines the number of ions available for the storage process, their mobility determines the maximum charging and discharging current. Both are limited. However, the current can be increased by connecting the strands in parallel. This also makes it possible to increase the amount of energy.

The circuit is described as $xpys$ interconnection. Here y is the number of cells connected in series and x for the parallel-connected strings of y cells.

For the design of a battery system, three factors must be coordinated with each other. The voltage window, the charging and discharging current and the total number of cells, i.e. the energy content of the battery.

3. Inverter technology

Most inverters in drive technology are based on the B6 topology (Figure 3). This topology consists of three half-bridges, each of which excites one phase. The switch on the upper half of the half-bridge generates the upper half-wave of the alternating current, the switch on the lower half of the half-bridge generates the lower half-wave.

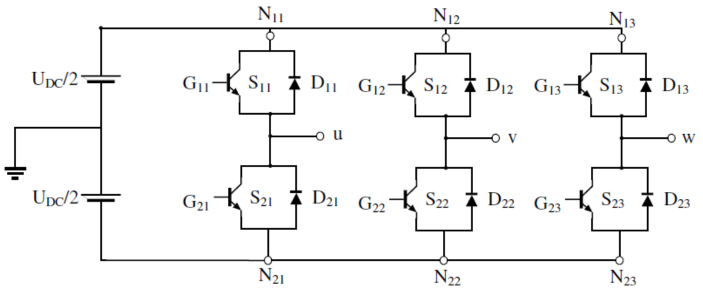

Figure 3 : Inverter circuit using a B6 topology. Three half-bridges are connected to a DC intermediate circuit. In this example, the DC voltage is tapped centrally. [4], [7]

The task of the inverter is to convert the battery's DC voltage into an AC voltage. The AC voltage should be such that the connected electric motor is able to generate a certain torque at a certain speed. The limitation in the inverter is the maximum permitted DC voltage and the maximum permitted current. Furthermore, a distinction is made between the continuous current and the peak current, which also allows a higher current load on the components for a short time. If one looks at the load profiles of mobile machines, it is noticeable that, compared to passenger cars, short-term peak loads occur much more frequently. [2], [3], [8]-[10]. Therefore, attention should be paid to this when selecting the inverter in order to avoid oversizing and thus additional costs.

4. Motor control

The core of the inverter software is the control. It contains the logic according to which the switches of the B6 bridge are used to set the three currents. $i_u(t), i_v(t), i_w(t)$ currents. In the static case, when constant alternating currents are present, we need four variables to describe the physics: The amplitudes of the alternating currents $\hat{\imath}_u, \hat{\imath}_v, \hat{\imath}_w$ and the time t. If we assume that the sum of the three alternating currents adds up to zero, we can reduce the number of descriptive variables to 3. If we now change to a coordinate system that rotates with the electric field in the motor, the number can be reduced to 2. This coordinate system is known as d,q-system.

In this study we consider the behaviour of permanently excited synchronous motors with buried magnets [11]. These motors are characterised by a high energy density and are used in various traction applications.

To understand the task of motor control, let us first consider the mathematical description of the motor in the d,q-system with the stator as the reference point.

$$u_{s,d} = R_s i_{s,d} + \frac{\mathrm{d}}{\mathrm{d}t}\psi_d - \omega_e\, \psi_q$$

$$u_{s,q} = R_s i_{s,q} + \frac{\mathrm{d}}{\mathrm{d}t}\psi_q + \omega_e \psi_d$$

$$\psi_d = L_d i_{s,d} + \psi_m$$

$$\psi_q = L_q i_{s,q}$$

$\psi_{d,q}$ are the magnetic fluxes that are generated by a current flow $i_{d,q}$ and the motor inductance $L_{d,q}$ result. In addition, the magnetic flux in d-direction is influenced by the magnetic flux of the magnets. ψ_m influenced.

The voltage $u_{s,(d,q)}$ are influenced by the magnetic flux and its temporal change, the time-independent influence depends on the speed of the motor. ω_e of the motor. Furthermore, the ohmic resistance influences R_s influences the voltage.

Two variables are relevant for the drive. The speed and the torque ω_e and the torque T. The speed can be adjusted by the control via an adaptation of the switching processes. The torque of the motor, on the other hand, is adjusted by the interaction between the currents and the magnetic flux:

$$T = \frac{3}{2} p \left(\psi_d i_{s,q} - \psi_q i_{s,d} \right)$$

It does not depend directly on the speed, but different pairs of i_d and i_q can set the same torque.

If a certain torque is to be set at a certain speed, the task of the control is to keep the losses as low as possible and to comply with two boundary conditions:

$$i_{s,d}^2 + i_{s,q}^2 \leq I_{\max}^2$$

$$u_{s,d}^2 + u_{s,q}^2 \leq U_{\max}^2$$

The first boundary condition is the current limit of the inverter and the motor. The second boundary condition describes the voltage limit given by the DC link voltage.

In Figure 4 the voltage and current limits as well as the torque curve are plotted for an example motor. The shape of the current limit corresponds to a circle in the d, q-coordinate system. The voltage limit of an ellipse. The torque curve of a hyperbola. Voltage limitation and torque curve depend on the motor parameters. To illustrate the fuzziness of these variables, which, with a variance of 5%, can be found in the variables L_q, L_d and ψ_m have been plotted in Figure 4. The uncertainty in the voltage is significantly higher than in the torque and increases sharply when the edge of the ellipse is reached.

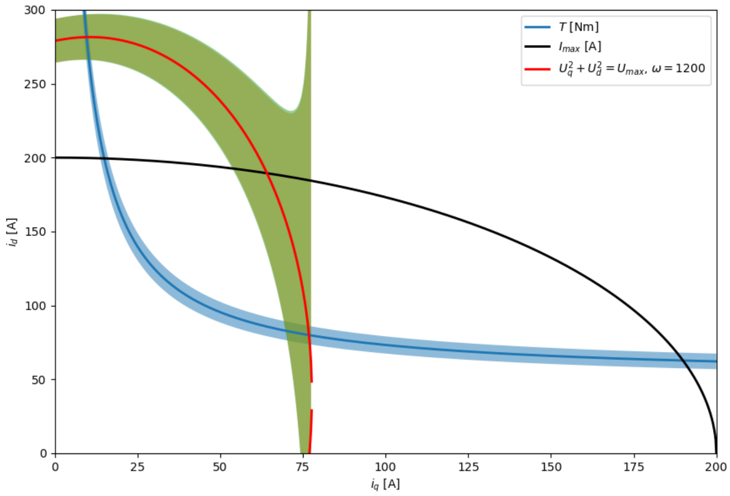

Figure 4 : Choice of d-current i_d as a function of i_q for a given torque, and the range of uncertainty when L_q, L_d and ψ_m are subject to a 5% error. Furthermore, the maximum current is entered. As well as the voltage limit and its uncertainty with a 5% error.

For the control system, the task is to find exactly that pair for a given torque. i_d, i_q-pair at which the total current is the lowest. Geometrically, this is equivalent to the question of which i_d, i_q-point has the shortest distance from the zero point. This type of control is called "Maximum Torque per Amp" (MTPA). In the left picture of Figure 5 shows this control case.

In Figure 5 the speed of the motor has been increased in each case. As can be seen, the radius of the voltage ellipse depends on the speed. The higher the speed, the smaller the radius. This is due to the $\pm\omega_e\psi_d$-term in the voltage equations.

In the middle picture, speed is too high that the point found for the MTPA is no longer within the ellipse. If the control would continue to drive the MTPA point, the voltage would exceed its limit and the inverter would go into fault. The control therefore tries to find a point with which it delivers the required torque and still complies with the voltage limit. Such a point exists in the constellation shown. This type of control is referred to as field weakening, because a higher electric field i_d the electric field generated by the motor is weakened.

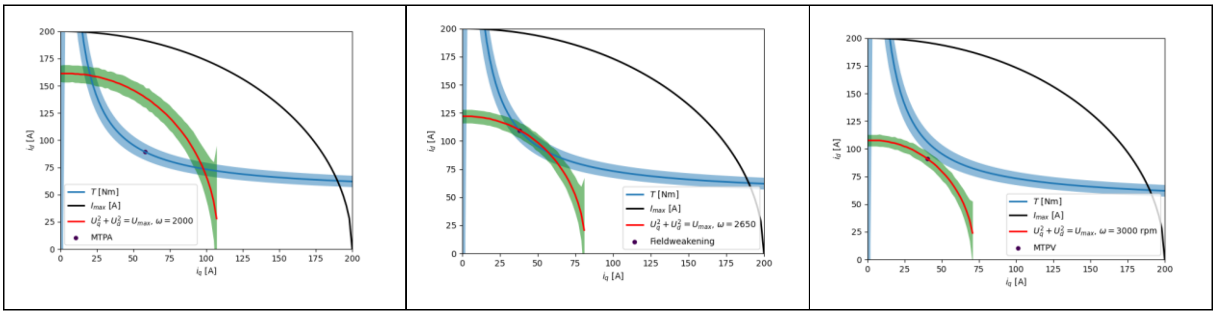

Figure 5 : In regulation, a distinction must be made between three cases. MTPA (left), field weakening (middle) and MTPV (right).

In the right image of Figure 5 now appears the case where the speed of the motor is so great that the radius of the voltage ellipse is so small that the torque curve no longer intersects it. There is no i_d, i_q-point that fulfils the torque and complies with the voltage limit. In such a case, the control tries to find the point that lies at the edge of the voltage ellipse and produces the greatest torque. This is called "Maximum Torque per Volt" (MTPV) control.

The radius of the voltage ellipse depends not only on the speed and other motor parameters, but also on the battery voltage. As we have seen, battery systems do not have a constant voltage, but have a voltage window that depends on the battery's state of charge (Figure 2). As a result, the ellipse of the voltage limit also changes not only with speed but also with battery voltage. In Figure 6 these are shown for an LFP battery. The voltage window for this battery lies between 450V and 650 V. With a fully charged battery, there is no difficulty for the control to call up the desired torque. With an (almost) discharged battery, however, it is no longer possible.

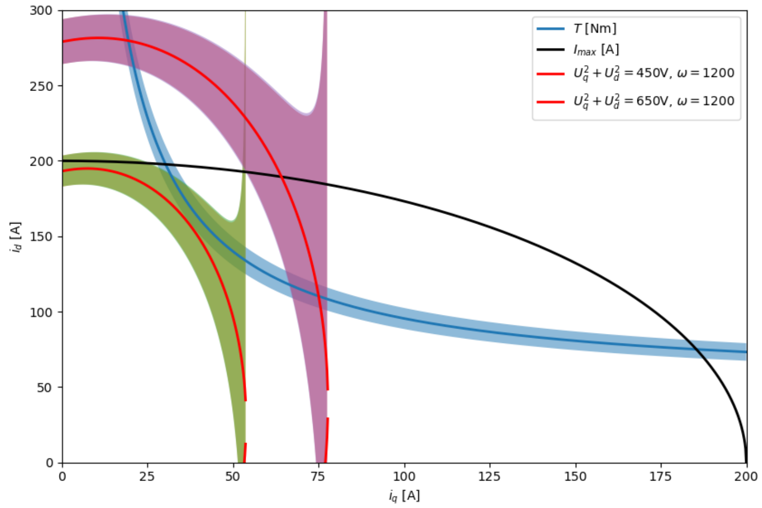

Figure 6 : Voltage limit ranges with different battery voltage and fuzziness. With a low battery voltage, the torque is in the fuzziness range of the voltage limit.

The effects of this state of charge dependency are shown in Figure 7 can be seen clearly. In this illustration, the operating limits of the motor were determined for each speed. The battery voltage was varied in the process. In both cases, up to $\omega = 2000\text{ rpm}$ the maximum torque can be reached. If the battery voltage is low, the control must already switch to MTPV control here. If the battery voltage is at 850 V the maximum torque can still be provided until $\omega = 3000\text{ rpm}$ can be provided.

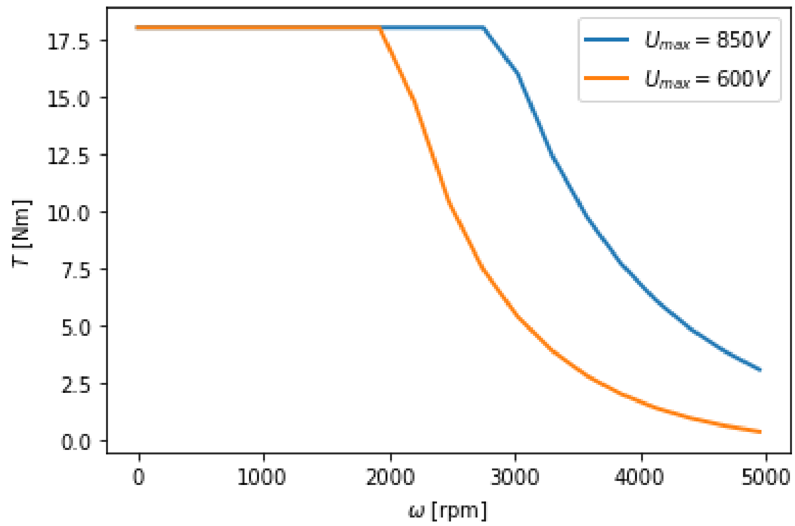

Figure 7 : Operating limits of the example motor at different battery voltages.

5. The hybrid-powered drivetrain

When designing the driveline, it must therefore be decided whether a power reduction at low battery voltage is acceptable or whether the system is designed for the minimum battery voltage. There are various ways to deal with this voltage-dependent power difference. For example, the motor train can be designed to refer to the low battery voltage. Or, using load profiles, one can look at the frequency of high torque and speeds and design the system to work well enough at low battery voltage. For mobile machines, such a power limitation does not always make sense, as high power is considerably more frequent than in other mobile applications.

As the battery voltage is the limiting element, a DC/DC controller between the battery and the inverter can alternatively compensate for the effect. In Figure 8 shows the two possible drive trains. The DC/DC controller is able to raise the battery voltage to the maximum voltage. The DC link voltage is therefore always constant. The voltage ellipse thus only depends on the speed. Another advantage is that the battery chemistry can be changed without altering the vehicle's behaviour. If the DC/DC controller is galvanically isolating, technical safety measures are partially omitted, which make the overall system more expensive and increase complexity.

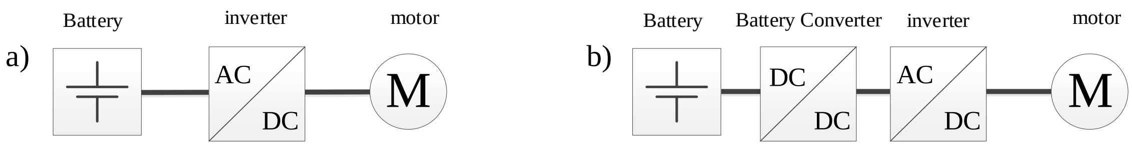

Figure 8 : Possible realisation of powertrains

The disadvantage of this in Figure 8 is that, on the one hand, a DC/DC converter means additional costs and, on the other hand, a DC/DC converter generates losses that may reduce the overall efficiency. In the following, we will deal with the aspect of overall efficiency, since any improvement in efficiency increases the range of the vehicle and can reduce the cost of the most expensive component, the battery.

To describe the efficiency, we need a simple model for the losses of the three components. In the previous studies, we had used a linear loss model as part of the system description through the power flow diagram. The power loss $P_L(P)$ was described by three loss coefficients:

$$P_L = a + b\,P + c\,P^2$$

This approach allowed a simple but quantitative comparison of different system solutions. To better describe the losses of the motor, inverter and DC/DC controller, we extend this approach to two degrees of freedom. The power loss $P_L(x, y)$ now depends on x and y in the case of the motor. In the case of the motor, it is torque and speed. In the case of the inverter and DC/DC controller, it is voltage and current. Here, too, we work with loss coefficients:

$$P_L(x,y) = a + b_x x + b_y y + b_{x,y} xy + c_x x^2 + c_y y^2$$

In Figure 9 shows the two-dimensional efficiencies for the DC/DC controller, inverter and motor. Their structure corresponds to real characteristic diagrams. However, the power limits were not taken into account in these representations. In Table 2 shows the loss coefficients used in this study. They are based on values of commercially available components.

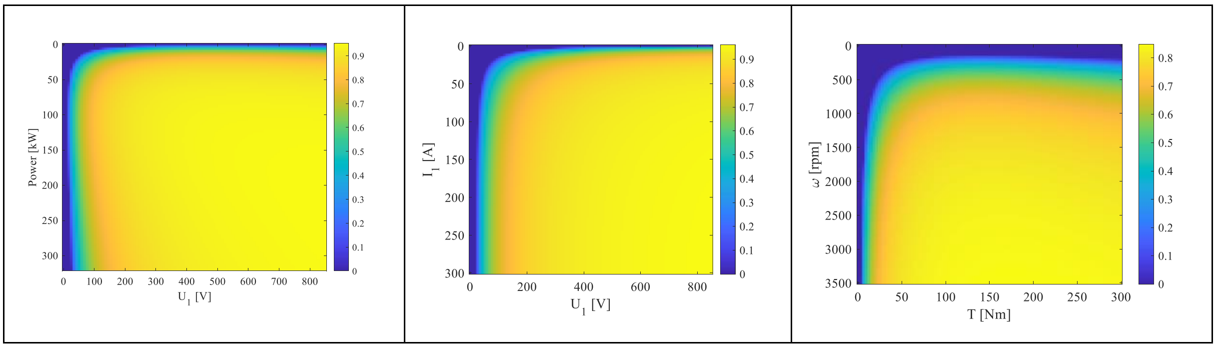

Figure 9 : Examples of efficiencies of DC/DC controller, inverter and motor.

Table 2 : Loss coefficients for DC/C controller, inverter and motor

$\eta_{\text{DC/DC}}$	$\eta_{\text{DC/AC}}$	η_{Motor}
$U_1^{\max} = 850\ \text{V}$	$U_1^{\max} = 850\ \text{V}$	$T^{\max} = 300\ \text{Nm}$
$I_1^{\max} = 300\ \text{A}$	$I_1^{\max} = 300\ \text{A}$	$\omega^{\max} = 4500\ \text{rpm}$
$a_0 = 1020\ \text{W}$	$a_0 = 153\ \text{W}$	$a_0 = 5775\ \text{W}$
$b_U = 2{,}82 \cdot 10^{-5}$	$b_U = 2{,}3 \cdot 10^{-4}\ \text{A}$	$b_T = 5{,}984\ \text{rpm}$
$b_I = 0{,}0074$	$b_I = 23{,}93\ \text{V}$	$b_\omega = 0\ \text{Nm}$
$b_{U,I} = 0$	$b_{U,I} = 0{,}0023$	$b_{T,\omega} = 0{,}0464$
$c_U = 0{,}0084 \frac{\text{A}}{\text{V}}$	$c_U = 0{,}00026 \frac{\text{A}}{\text{V}}$	$c_T = 0{,}0594 \frac{\text{rpm}}{\text{Nm}}$
$c_I = 0{,}0227 \frac{\text{V}}{\text{A}}$	$c_I = 0{,}00097 \frac{\text{V}}{\text{A}}$	$c_\omega = 0{,}0043 \frac{\text{Nm}}{\text{rpm}}$

To determine the overall efficiency $\eta(T, \omega, U_B)$ we proceed in such a way that we first determine the motor losses at a certain operating point. (T, ω) are determined.

The motor power that is required is

$$P_{\text{IM}} = T\omega$$

The power that the inverter must provide results in:

$$P_{\text{inv}} = \frac{P_M}{\eta_M(T,\omega)}$$

The current required for this on the primary side of the inverter is

$$I_{AC,1} = \frac{P_M}{\eta(T,\omega)U_B}$$

If we use a DC/DC controller, the required current would be on the primary side of the inverter:

$$I_{AC,1} = \frac{P_M}{\eta(T,\omega)U_{DC}}$$

Where U_{DC} is the optimum DC link voltage for the inverter.

In Figure 10 shows the efficiencies with and without DC/DC converter for three operating points. Without the DC/DC controller, there is a clear drop in efficiency of about 2% over the entire voltage range shown. If we look at the voltage windows of LFP or NMC, the drop is smaller, but still clearly visible. And it should not be forgotten here that at lower voltages not all operating points can be operated.

If a DC/DC controller is used, the following can be seen in Figure 10that the efficiency remains constant. At high voltages, the use of the DC/DC converter is somewhat worse. This is because the losses of the DC/DC converter are added. If one takes into account that the use of a DC/DC converter also makes the operating range of the motor independent of the battery state of charge, there is a lot to be said for the use of a DC/DC converter in this case.

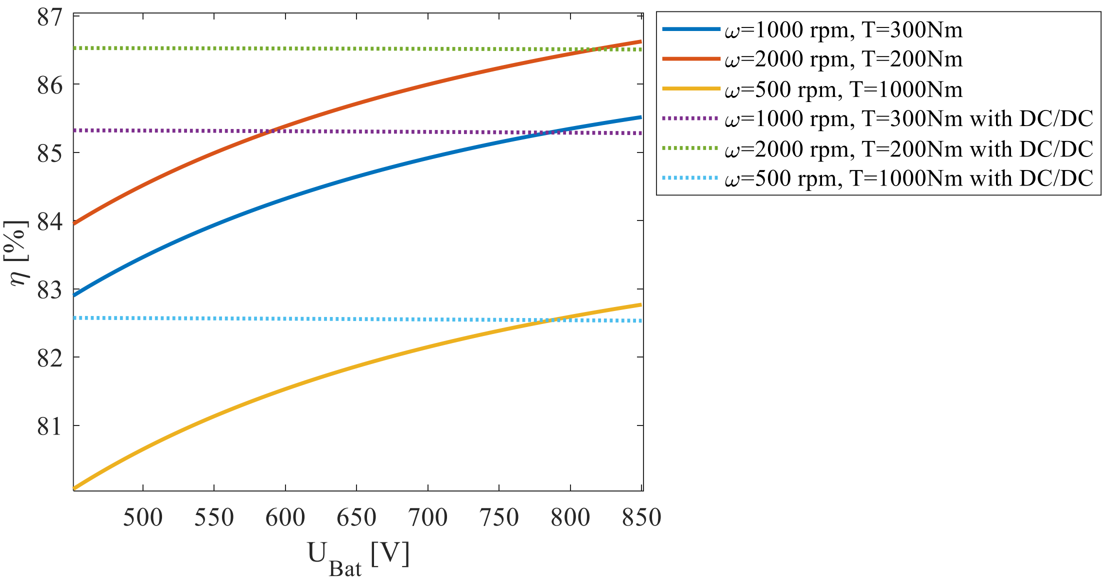

Figure 10 : Overall efficiency of the drive train at different operating points with and without DC/DC controller.

6. Summary

In this study, we looked at the triad of battery, inverter and motor. We have seen that the choice of battery has an influence on the performance of the motor. We did not take a closer look at aspects such as the maximum charging and discharging rate or battery ageing. These also have an influence on the design of the overall system. In particular, cycle ageing and calendar ageing of the battery have a significant influence on the total cost of ownership. [4], [6], [12], [13].

When controlling the motor, a distinction can be made between three operating modes: Maximum torque per amp, field weakening and maximum torque per volt. Which control is used depends on the speed, battery voltage and other motor characteristics of a permanently excited motor.

We have also been able to show that this triad can be weakened by integrating a DC/DC converter. The power supply of the inverter becomes independent of the battery voltage. We were also able to show that the additional losses do not have to be so high and that the benefit of the overall system can be higher.

For the electrification of mobile machines, these results mean that after a consideration of the power flow diagram and initial topology decisions, the characteristics of the drive train must be looked at more closely. And that great savings potentials can be identified here at both system and component level.

References

[1] Armin U. Schmiegel, "From the smoking exhaust to the clean socket Design steps from the diesel-powered mobile machine to the all-electric mobile machine Part 1 - Power and Energyconsiderations," Reutlingen, 2022.

[2] A. U. Schmiegel, "Design consideration for a hybrid Fuel cell truck," 2022.

[3] Armin U. Schmiegel, "The Straddle Carrier as an example for the electrification of mobile machines," Reutlingen, 2022.

[4] A. U. Schmiegel, *Energy Storage Systems,* vol. in Press. Oxfort: Oxfort University Press, 2022.

[5] A. A. Akhil *et al*, "DOE / EPRI 2013 Electricity Storage Handbook in Collaboration with NRECA," no. July, 2013.

[6] A. U. Schmiegel, *Energiespeicher für die Energiewende*. Munich: Hanserverlag, 2019.

[7] B. Erickson, "Introduction to Power Electronics," in *Computer Engineering*.

[8] A. Lajunen, P. Sainio, L. Laurila, J. Pippuri-Mäkeläinen, and K. Tammi, "Overview of powertrain electrification and future scenarios for non-road mobile machinery," *Energies,* vol. 11, no. 5. MDPI AG, 2018. doi: 10.3390/en11051184.

[9] A. Lajunen, J. Suomela, J. Pippuri, K. Tammi, T. Lehmuspelto, and P. Sainio, "Electric and hybrid electric non-road mobile machinery-present situation and future trends," Jun. 2016, [Online]. Available: http://www.rocla.com

[10] J. Kukkaro, "Straddle Carrier Electric Powertrain Optimization," no. August, 2016.

[11] C. Capitan, "Torque Control in Field Weakening Mode," Aalborg University, 2009.

[12] D. Hoog *et al*, "Aging phenomena for Lithium-Ion batteries," 2014.

[13] P. Keil and A. Jossen, "Aging of lithium-ion batteries in electric vehicles:," *Dissertation*, vol. 7, no. 1, pp. 41-51, 2017.